

Electron correlation effects in the half-metallic NiMnSb within a cluster-perturbation approach with ab-initio parameters

H Allmaier¹, L Chioncel^{1,2}, E Arrigoni¹, M I Katsnelson³, A I Lichtenstein⁴

1. Institute of Theoretical Physics, Graz University of Technology, A-8010 Graz, Austria

E-mail : hannes.allmaier@itp.tugraz.at

2. Faculty of Science, University of Oradea, RO-47800, Romania

3. Institute for Molecules and Materials, Radboud University of Nijmegen, NL-6525 ED Nijmegen, Netherlands

4. Institute of Theoretical Physics, University of Hamburg, 20355 Hamburg, Germany

(Received 25 January 2008)

Abstract

Using a combination of electronic-structure and many-body calculations, we investigate correlations effects in the halfmetallic ferromagnet NiMnSb. A realistic many-body Hamiltonian, containing only Mn-d orbitals shows the importance of non-quasiparticle states just above the Fermi level. Our results suggest that for a better description of low energy states around Fermi level, Ni-d orbitals should be explicitly included.

Keywords: half metal, cluster perturbation, electron correlation

1. Introduction

Since the prediction of half-metallic ferromagnetism by de Groot et al. [1] more than twenty years ago, the physics of these materials has attracted a great deal of interest. Ideally, half-metallic compounds should show metallic behaviour for one spin channel, and a perfect insulating behaviour for the other spin direction. This special property is of high interest in spintronics, a recently developed branch of electronics where not only the charge but also the spin is manipulated. Consequently, in a perfect half-metallic ferromagnet one would expect to find a gap in one spin channel. However, complete spin polarization has not been found experimentally yet. Although values as high as 96 % have been reported for CrO₂, spin polarization is usually significantly smaller in other compounds. For example, in NiMnSb values between 40-60 % were reported [2,3]. Various reasons have been invoked for this drastic depolarization, ranging from surface and interface effects at T=0 [4], and more recently finite temperatures correlation effects leading to formation of non-quasiparticle states with significant spectral weight at the Fermi-energy [5-7].

In general, spintronic devices will have to operate at room temperature, so compounds with high Curie

temperatures and at the same time high magnetisations are of interest. Among other materials, the prototype half-metallic ferromagnet NiMnSb having $T_c = 730\text{K}$ and $M_s = 4\mu_B$ is an attractive candidate for which the physics of the spin polarization have to be understood. In order to investigate the relevant physics of NiMnSb it is important to start from a realistic Hamiltonian.

Following our previous results [8], starting from realistic band-structure calculations we first derive by downfolding [9,10] an effective Hamiltonian acting on the Mn d-orbitals only. The obtained model Hamiltonian, which includes explicitly the electron-electron interaction, is solved using the Cluster Perturbation Theory approach which accounts for many-body effects on the lattice. Based on the results of our combined electronic and many-body calculation, we suggest that the additional orbital degrees of freedom of the Ni-d orbitals should be included in the Hamiltonian in order to give a proper description for the minority spin gap in NiMnSb.

In section 2, we give a brief introduction of the crystal and electronic structure for NiMnSb within the framework of Density Functional Theory in the Local Density Approximation. Bands obtained using the NMTO downfolding technique are presented and

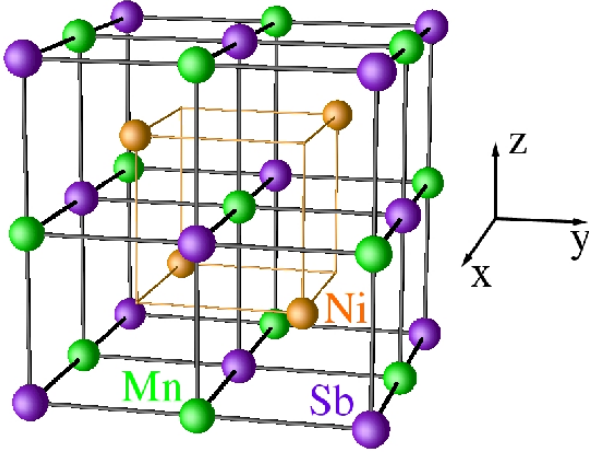


Figure 1. (Color online) Structure of the semi-Heusler compound NiMnSb: Mn (green) located at $(0,0,0)$ and Sb (purple) located at $(\frac{1}{2}, \frac{1}{2}, \frac{1}{2})$ form the rock salt structure. Ni (orange) sits at the octahedrally coordinated pocket at one of the cube center positions $(\frac{3}{4}, \frac{3}{4}, \frac{3}{4})$ and creates holes in the structure by leaving the other $(\frac{1}{4}, \frac{1}{4}, \frac{1}{4})$ empty.

discussed. The many-body Hamiltonian which supplements the non-interacting realistic Hamiltonian obtained through LDA-NMTO is presented in section 3. Sec. 4 describes the methodology used in order to solve the many-body problem, namely the Cluster Perturbation Theory approach. The results are presented in section 5, and the last section summarizes our results.

2. Electronic structure of the NiMnSb crystal

The intermetallic compound NiMnSb crystallizes in the cubic structure of MgAgAs type (CI_b) with the *fcc* Bravais lattice (space group $F\bar{4}3m = T_d^2$). The crystal structure is shown in Fig. 1. This structure can be described as three interpenetrating fcc lattices of Ni, Mn and Sb. The Ni and Sb sublattices are shifted relative to the Mn sublattice by a quarter of the $[111]$ diagonal in opposite directions.

A detailed description of the band structure of semi-Heusler alloys has been previously carried out by means of electronic structure calculations and tight-binding model analysis [1,11-14]. Here, we briefly summarize the results. The important aspects which determine the behavior of the electrons near the Fermi level and the half-metallic properties are the interplay between the crystal structure, the valence electron count, the covalent bonding, and the large exchange splitting of the *Mn-d* electrons.

The electronic band structure of NiMnSb is presented in Fig. 2. For the minority spin gap opening, not only the *Mn-d*-*Sb-p* interactions, but also *Mn-d*-*Ni-d* interactions have to be taken into account. In addition, the loss of inversion symmetry produced by the CI_b structure (the symmetry lowering from O_h in the $L2_1$ structure to T_d in the CI_b structure at *Mn* site)

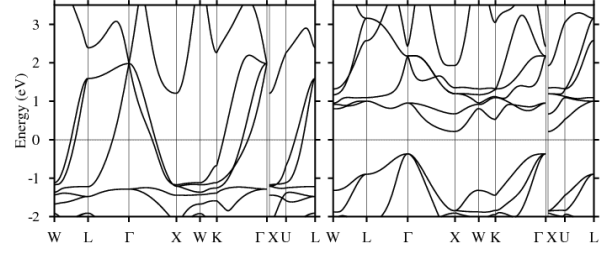


Figure 2. Full basis set spin-polarized (ferromagnetic) bands for NiMnSb; majority spin (left) and minority spin (right).

contributes essentially. The existence of *sp*-valent *Sb* is crucial to provide stability to this compound.

As a first step, and based on the bonding picture in *NiMnSb* briefly described above, we used a downfolding scheme in which all orbitals of all atoms except *Mn-d* are downfolded [8]. The downfolding procedure uses the NMTO method [9,10] to generate truly minimal basis sets. Downfolding produces minimal bands which follow exactly the bands obtained with the full basis set. As a first approximation, we only keep *Mn-d* orbitals in this minimal basis set. The minimal set of symmetrically orthonormalized NMTOs is a set of Wannier functions. In the construction of the NMTO basis set the active channels are forced to be localized onto the eigenchannel, $\mathbf{R}|m$ therefore the NMTO basis set is strongly localized.

Fourier transformation of the orthonormalized NMTO Hamiltonian, $H^{LDA}(k)$, yields on-site energies and hopping integrals,

$$H_{0m', \mathbf{R}m}^{LDA} \equiv \left\langle \chi_{0m}^\perp \left| \mathcal{H}^{LDA} - \varepsilon_F \right| \chi_{\mathbf{R}m}^\perp \right\rangle \equiv t_{m', m}^{xyz} \quad (1)$$

in a Wannier representation, where the NMTO Wannier functions $|\chi_{\mathbf{R}m}^\perp\rangle$ are orthonormal.

The matrix element between orbitals c and m on the same site $\mathbf{R}' = \mathbf{R} = \mathbf{0}$ is referred to as $t_{m', m}^0$, while the hopping integral from orbital m' on site $\mathbf{R}' = \mathbf{0}$ to orbital m on site $\mathbf{R} = (x, y, z)$ is called $t_{m', m}^{xyz}$. Further information concerning the matrix elements or technical details of the calculation can be found in Ref. [8].

In the construction of the many-body Hamiltonian the *Mn* t_{2g} and e_g orbitals were considered as *active orbitals* responsible for the low energy physics of NiMnSb.

3. Model Hamiltonian and parameters

To investigate the correlations in NiMnSb we employ the multi-orbital Hubbard-model:

$$H_0 = \sum_{i \langle m, \sigma \rangle} t_{im\sigma, jm'\sigma} c_{im\sigma}^\dagger c_{jm'\sigma}, \quad (2)$$

$$H_I = \frac{1}{2} \sum_{i, m, \sigma} U_{mmmm} n_{im\sigma} n_{im-\sigma}, \quad (3)$$

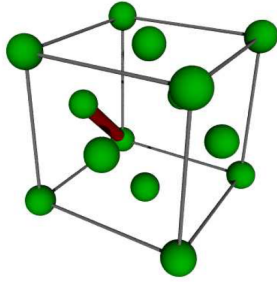


Figure 3. (color online) Description of the lattice used for the CPT-calculation. The thick line (in red) denotes one cluster, which is repeated periodically in the lattice. Note that due to the downfolding procedure only the Mn-sublattice is considered.

$$+\frac{1}{2} \sum_{i,m \neq m'} (U_{mm'mm'} - \frac{1}{2} J_{mm'mm'}) n_{im} n_{im'} \quad (4)$$

$$- \sum_{i,m \neq m'} S_{im} S_{im'}, \quad (5)$$

where $t_{im\sigma, jm'\sigma}$ denotes the coefficient of the hopping process between orbitals m, m' at sites, i, j respectively.

$c_{im\sigma}^\dagger$ and $c_{im\sigma}$ are the usual fermionic creation and annihilation operators applied to an electron with spin σ at site i in the orbital m . In this form, the Hamiltonian also considers Coulomb interaction between different orbitals, for both electrons with parallel and anti-parallel spin orientations. Spin- and pair flip terms are also taken into account.

For the bare (unscreened) Coulomb interaction we chose intermediate values: $U = 3.0\text{eV}$ and $J = 0.9\text{eV}$, in agreement with previous work [5, 15-17].

4. Cluster perturbation theory

Cluster Perturbation Theory (CPT) [18,19] is a technique to approximate the single-particle Greensfunction of strongly correlated systems. It takes into account short range correlations on the length scale of the cluster by using exact diagonalization. Intercluster hoppings are taken into account by strong-coupling perturbation, leading to an approximation for the lattice Greens function. This approximation becomes exact in following limits: for an infinite cluster, in the uncorrelated case, $U = 0$, and in the atomic limit, $t = 0$ (more exactly in the limit of no inter-cluster hoppings).

The procedure consists in splitting the Hamiltonian into a cluster and an inter-cluster component $H = H_{cl} + T_{cl-cl}$. Accordingly, the hoppings are divided into intracluster (the red line in Fig. 3) and inter-cluster terms (T).

Within the cluster, the Greens function G_{cl} is calculated numerically using a zero-temperature Lanczos procedure, as a function of frequency, spin and orbital indices. The CPT Greensfunction can be expressed in terms of the decoupled clusters Greensfunction and the inter-cluster hopping matrix elements: $G_{CPT}^{-1} = G_{cl}^{-1} - T$.

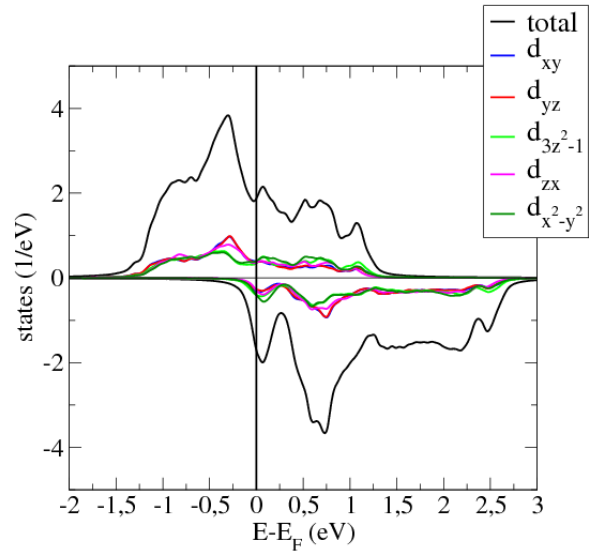


Figure 4. (Color online) CPT-results for NiMnSb using the Mn only NMTO-basis set; a screened Coulomb interaction ($U = 0.75\text{eV}, J = 0.9\text{eV}$) was used (see text).

In this way, intercluster hopping processes neglected in the Lanczos calculation are taken into account. For the present CPT calculation we used a simple cluster consisting of two Mn-sites as reference system, as depicted in Fig. 3.

5. LDA+CPT-results

The present calculations only considers Mn in the NMTO-basis set. As described in Section 2, Ni-3d electrons on the one hand contribute essentially to the bonding of NiMnSb, and on the other hand play an important role in screening the local Coulomb interactions. The evaluation of the Coulomb matrix elements is a rather complicated task and beyond the scope of the present paper. By analyzing the band structure using the so-called "fatband" representation of the NMTO-code, we deduced an average screening factor of approx. 0.4 around the Fermi-energy. This leads to a reduced value of $U = 0.75$. For the exchange Coulomb parameter we choose accordingly a value of $J = 0.23\text{eV}$.

In contrast to a previous work [20] we diagonalize the cluster in the fully polarized sector, which is the most stable one. For the cluster this gives a magnetization of $4 \mu_B$. However, the intercluster hopping terms included via CPT and the consequent appearance of states in the minority spin band at the Fermi energy reduce the spin-polarization drastically to about $3 \mu_B$.

The density of states obtained from the LDA+CPT calculation is displayed in Fig.4. A resonance, due to many-body effects is clearly seen in both spin bands at about 0.1eV. This effect is connected to the existence on non-quasiparticle states, occurring just above the Fermi level. The tail of these states crosses the Fermi energy and produces a drastic depolarization. Similar NQP states were obtained for a one-band Bethe lattice model [5]

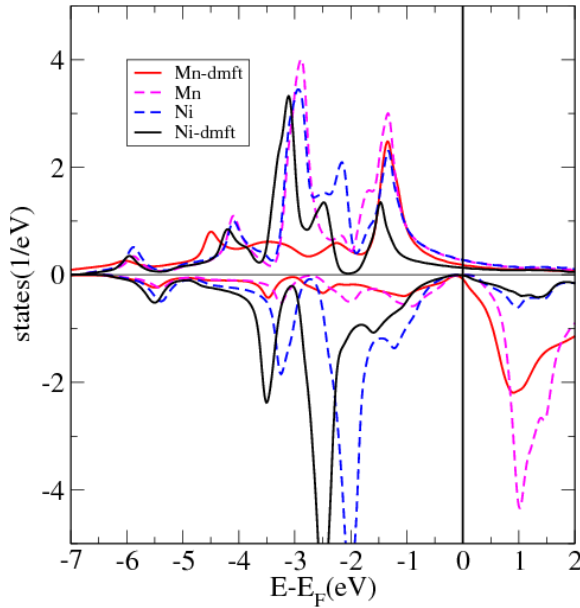


Figure 5. (Color online) Density of states for NiMnSb using Dynamical Mean field Theory (DMFT)[5] for $U = 3.0\text{eV}$, $J = 0.9\text{eV}$. The LSDA-DOS is plotted for comparison

solved using a Quantum Monte-Carlo solver of the DMFT problem.

The bandwidth of the Mn- d bands extends in a region of $\pm 3\text{eV}$. This is partly due to the downfolding procedure, which only keeps the Mn- d orbitals, and also because the screened U Coulomb parameter has a reduced value. It is instructive to compare the features of the LDA+CPT density of states with the results of a previous LDA+DMFT calculation [5]. While the former only takes into account the Mn orbitals, the latter accounts also for the presence of all other orbitals belonging to the atoms within the unit cell. Even though the obtained density of states shows significant differences, a qualitative agreement exists.

In Figs. 5 and 6, the total and partial (projected on Mn, Ni) density of states obtained using a LDA+DMFT scheme are displayed. In contrast to the uncorrelated LSDA calculation, the DMFT results show the existence of NQP states. However, their position and spectral weight is different from the CPT results.

In a direct comparison of the majority spin band, we find that the LSDA-DOS shows a structure at about -1.5eV which is already slightly shifted up to Fermi energy in the DMFT-DOS. In CPT this structure is further shifted to Fermi energy by about 0.5eV and one finds also more states at and above Fermi energy. In the minority spin band the CPT results show no states below Fermi energy, which is as expected since we start from the fully polarized state, where the minority spin band is

empty. This result is similar to the ones obtained for a Bethe-lattice model [5], where the minority spin gap was obtained using a fictitious ferromagnetic-type field which mimicked the local Hund polarization originated from other orbitals. Since in the LDA+CPT calculations the full Mn- d manifold is taken into account such a fictitious field is not required.

In order to be able to address the issue of polarization in NiMnSb, occupied minority states should be included in the calculation, this can be achieved by including Ni- $3d$ orbitals in the model Hamiltonian. As a matter of fact, the downfolding procedure indicates that Ni lies energetically deep below the Fermi energy (-3eV to about -1eV). Nevertheless, its influence to the electronic structure around the Fermi energy might be important. Therefore, a possible extension of the present calculation would be the inclusion of Ni- $3d$ orbitals into the NMTO-basis set, and consequently into CPT. Preliminary results show a significant improvement of LDA+CPT density of states as compared to the DMFT results. Therefore, we suggest that the processes related to the suppression of spin polarization could be more realistically described by an inclusion of Ni orbitals. A further advantage of this would be that one could use the bare Coulomb interaction without resorting to the average screening approximation used here.

Finally, we investigated to which extent the choice of only two sites for the reference system influences the results, since a significant number of hopping processes are not directly taken into exact diagonalization. However, test calculations for a 4-site fully-polarised cluster show that only the fine structure of the DOS changes, while its general shape remains to a large extent unmodified.

6. Summary and conclusions

Using a combined LDA+CPT approach with an effective Hamiltonian projected to the Mn- d orbitals, we have investigated the effects of correlations in NiMnSb. Our results show the existence of non-quasiparticle states just above the Fermi level in agreement with previous model calculations such as the Bethe lattice or LDA+DMFT.

Our calculations also show that although Mn accounts for the important excitations close to the Fermi energy, Ni d -orbitals should be considered as well in order to access the full nature of NiMnSb, especially around the Fermi energy. Future work will address this point, since it is of special importance for the understanding of depolarization effects as a function of temperature.

We acknowledge financial support by the Austrian science fund (FWF project P18505-N16).

References

1. R A de Groot et al., *Phys. Rev. Lett.* **50** (1983) 2024.
2. R J Soulen et al., *Science* **282** (1998) 85.
3. S K Clowes et al., *Phys. Rev. B* **69** (2004) 214425.
4. G A de Wijs and R A de Groot, *Phys. Rev. B* **64** (2001) 020402.
5. L Chioncel, M I Katsnelson, R A de Groot, and A I

- Lichtenstein, *Phys. Rev. B* (Condensed Matter and Materials Physics) **68** (2003) 144425.
6. L Chioncel et al., *Phys. Rev. B* **75** (2007) 140406.
 7. L Chioncel et al., arXiv:0711.2476 (unpublished).
 8. A Yamasaki, L Chioncel, A I Lichtenstein, and O K Andersen, *Phys. Rev. B* **74** (2006) 024419.
 9. O K Andersen and T Saha-Dasgupta, *Phys. Rev. B* **62** (2000) R16219.
 10. E Zurek, O Jepsen, and O K Andersen, *Chem Phys Chem* **6** (2005) 1934.
 11. S Ögüt and K M Rabe, *Phys. Rev. B* **51** (1995) 10443.
 12. I Galanakis, P H Dederichs, and N Papanikolaou, *Phys. Rev. B* **66** (2002) 134428.
 13. B R K Nanda and I Dasgupta, *Computational Materials Science* **36** (2006).
 14. E Kulatov and I I Mazin, *J. Phys.: Condens. Matter* **2** (1990) 343.
 15. L Chioncel et al., *Phys. Rev. B* **71** (2005) 085111.
 16. L Chioncel, E Arrigoni, M I Katsnelson, and A I Lichtenstein, *Phys. Rev. Lett.* **96** (2006) 137203.
 17. L Chioncel et al., *Phys. Rev. Lett.* **96** (2006) 197203.
 18. C Gros and R Valenti, *Phys. Rev. B* **48** (1993) 418.
 19. D S'en'echal, D Perez, and D. Plouffe, *Phys. Rev. B* **66** (2002) 075129.
 20. H Allmaier, L Chioncel and E Arrigoni, *Journal of Optoelectronics and Advanced Materials* (JOAM) **10** (2008) 7.